ELEKTRYKA 2016
Zeszyt 1 (237) Rok LXII

Janusz HETMAŃCZYK, Krzysztof KRYKOWSKI, Antoni SKOĆ
Silesian University of Technology

MECHANICAL RESONANCE IN HIGH SPEED PERMANENT MAGNET BRUSHLESS DC MOTOR

Summary. The paper presents how to determine the ranges of rotational speeds for high-speed brushless DC motors (PM BLDC), in which the mechanical resonance caused by flexural and torsional vibrations occurs. In the comparative analysis real measurement data of the developed high-speed PM BLDC motors have been used. Presented results of a laboratory experiment confirmed the correctness of the method of calculation of resonance occurrence in PM BLDC motor.

Keywords: High-speed permanent magnet brushless DC motor (PM BLDC), mechanical resonance, flexural and torsional vibrations

REZONANS MECHANICZNY W WYSOKOOBROTOWYM BEZSZCZOTKOWYM SILNIKU PRĄDU STAŁEGO

Streszczenie. W artykule przedstawiono sposób wyznaczenia zakresów prędkości obrotowych dla wysokoobrotowych bezszczotkowych silników prądu stałego (PM BLDC), w których występuje rezonans mechanicznych drgań giętnych i skrętnych. W analizie porównawczej wykorzystano rzeczywiste dane opracowanych wysokoobrotowych silników PM BLDC. Przedstawiono wyniki eksperymentu laboratoryjnego potwierdzające poprawność sposobu obliczeń wstępowania rezonansów w silniku PM BLDC.

Słowa kluczowe: Wysokoobrotowy bezszczotkowy silnik prądu stałego (PM BLDC), rezonans mechaniczny, drgania giętne i skrętne

1. INTRODUCTION

Lots of engineering processes require application of high speed drives, i.e. drives rotating at high speeds [4]. Ideal high-speed motor should be characterized by high efficiency, small size, small moment of inertia and its operation should be stable as to mechanical vibrations, while the emitted noise should be low [2, 3]. Brushless dc motor (PM BLDC) fulfils these requirements. Principle of operation of high-speed motor is the same as in other types of PM BLDC motors [6]. Wiring diagram for main circuit of three-phase PM BLDC motor with star-connected windings and 3-phase bridge electronic commutator is shown in Fig.1. In case of

high speed motors designs with one pair of poles are recommended. The different phase windings are sequentially switched on by bridge transistors; they generate magnetic field and vector of this field may assume six different positions.

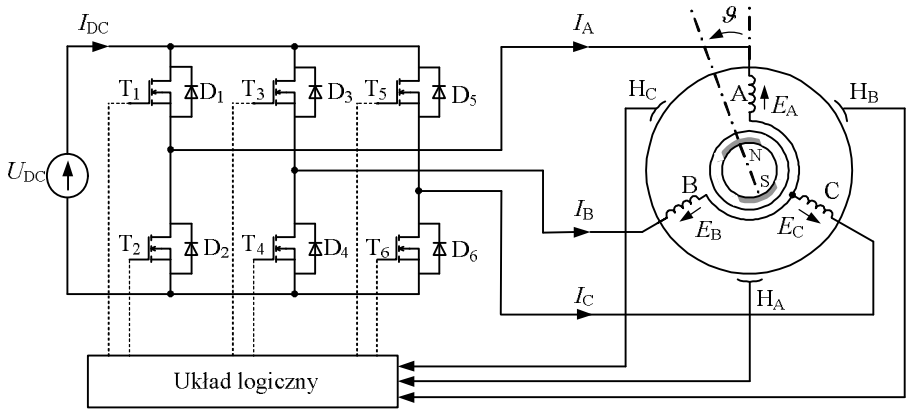

Fig. 1. Wiring diagram for 3-phase PM BLDC motor with electronic commutator
Rys. 1. Schemat połączeń 3-fazowego silnika PM BLDC z komutatorem elektronicznym

Rotors of high-speed electric motors are among those most prone to dynamic strain. In particular operation in resonance range is hazardous, since vibration amplitudes there usually attain unacceptable values, which in turn cause damage of rotors, bearings or couplings [3].

Resonance is present when frequency of forced vibrations is equal or is a multiple of the natural frequency of the rotor. Rotor's natural frequency depends on its size and placement of masses, method of support and its elastic properties [7]. Frequency of forced vibrations depends on the input frequencies, which may be caused by:

- periodically variable tangential forces or torsional torques causing torsional vibrations,
- periodically variable transverse forces causing flexural vibrations,
- periodically variable longitudinal forces causing longitudinal vibrations.

Frequency of rotor's longitudinal natural vibrations is usually very high and practically it is not present in motors. Resonance of torsional vibrations may occur in some machines with distinctly variable torque curves, such as piston engines or electric motors. On the other hand, flexural vibrations may occur in almost every machine (motor). This is due to demand for continuous decrease of machine (motor) size as well as ongoing increase in rotational speeds in modern machines. In this way rotor's (shaft's) natural vibration frequency decreases, while forced vibration frequency increases. These two quantities tend to approach each other, which may give rise to dangerous flexural vibration resonance in electric motors [7].

In the following sections of the paper we shall present a method of theoretical calculation of those rotational speed ranges, where mechanical resonance of flexural and torsional vibrations may take place. Results of calculations for two high-speed PM BLDC motors will be presented to justify correctness of the proposed method. In the discussion of torsional and flexural vibration issues we have neglected the impact of damping.

2. ROTOR'S FLEXURAL VIBRATIONS

The rotor of any electric motor is subjected to centrifugal forces of inertia due to even insignificant eccentricity of centre of gravity of rotating mass in relation to rotational axis (Fig.3) [3, 7]. For angular speed ω, centrifugal force F will generate (at the point of application of force) the dynamic deflection of rotor axis equal to y. The maximum rotation radius of centre of gravity of mass located at element's rotor (Fig.2) , taking into account rotor's eccentricity e is equal to:

$$r = y + e \tag{1}$$

Therefore, centrifugal force may be expressed as:

$$F = m \cdot \omega^2 r = m \cdot \omega^2 (y + e) \tag{2}$$

This force is balanced by elasticity force proportional to dynamic deflection of the shaft:

$$F^* = y \cdot c_g \tag{3}$$

where c_g is flexural rigidity of the shaft (force causing a per unit deflection).

When forces F and F^* are compared, we obtain a relationship describing dynamic deflection of the shaft in the plane where centrifugal force acts:

$$y = \frac{e}{\frac{c_g}{m \cdot \omega^2} - 1} = \frac{e}{\left(\frac{\omega_o}{\omega}\right)^2 - 1} \tag{4}$$

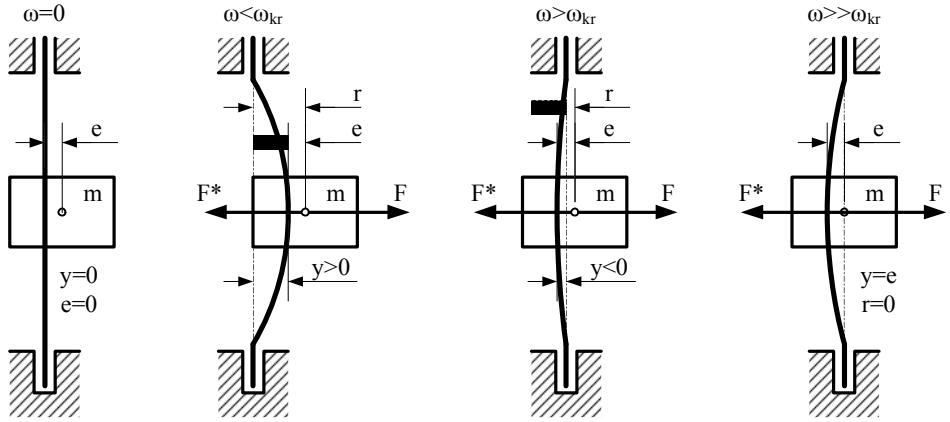

Fig. 2. Dynamic deflection of rotor shaft: a) immobile rotor, b) rotor speed less than critical, c) rotor velocity exceeding critical value ; $\omega > \omega_{kr}$, d) stable operation of rotor, $\omega >> \omega_{kr}$

Rys. 2. Dynamiczne ugięcie wału wirnika: a) wirnik w spoczynku, b) obroty wirnika mniejsze od krytycznych, c) obroty wirnika przekroczyły wartość krytyczną; $\omega > \omega_{kr}$, d) wirnik w stanie stabilnej pracy $\omega >> \omega_{kr}$

It is easily observed that dynamic deflection of the rotor shaft approaches infinity when $\omega^2 = c_g/m$. Angular speed of the rotor at which the deflection increases infinitely, is called *critical frequency*. Theory of vibrations [7] shows that frequency of transverse vibrations of the system presented in Fig.2 is equal to frequency of natural vibrations:

$$\omega_{kr} = \omega_o = \sqrt{\frac{c_g}{m}} \tag{5}$$

In order to determine critical speed of the shaft, we must first calculate the rotor deflection $y_{(F)}$ at the point of application of any static transverse force F^*, and then calculate shaft rigidity:

$$c_g = \frac{F^*}{y_{(F)}} \tag{6}$$

When (6) is substituted into (5), we obtain:

$$\omega_{kr} = \sqrt{\frac{F^*}{m \cdot y_{(F)}}} \tag{7}$$

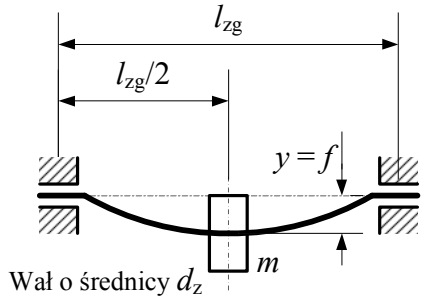

Fig. 3. The scheme of equivalent rotor shaft and its deflection caused by centrifugal force appearing as a result of rotation of mass denoted as *m*
Rys. 3. Schemat wału zastępczego wirnika i jego ugięcie pod wpływem działania siły odśrodkowej pojawiającej się w wyniku wirowania masy *m*

Motor shaft is loaded with transverse force *F* (Fig. 3), resulting from action of centrifugal force. Rotor deflection *f* and air gap *e** are related in the following way: *e**>*f*. However:

$$y = \frac{F \cdot l_{gz} \cdot a^2}{6 \cdot E \cdot I} \tag{8}$$

where:

I – moment of inertia of motor's rotor, which is equal to:

$$I = \frac{\pi \cdot d_z^4}{64} \tag{9}$$

E – Young's modulus, for steel $E = 2.1 \cdot 10^5$ MPa,

a – distance between rotor supports,

l_{gz} – equivalent length of shaft for a rotor with stepped shaft(Fig. 4):

$$l_{gz} = 2 \cdot l_1 \left(\frac{d_z}{d_1}\right)^4 + 2 \cdot l_2 \left(\frac{d_z}{d_2}\right)^4 + l_3 \left(\frac{d_z}{d_3}\right)^4 \tag{10}$$

In case of machine shafts [3], and on account of critical speed, steady-state operation of rotor shaft in the range of speeds defined by (11) must be avoided:

$$0.85 \cdot n_{gkr} \geq n \geq 1.15 \cdot n_{gkr} \tag{11}$$

where critical speed expressed in rpm is equal to:

$$n_{gkr} = \frac{30}{\pi}\omega_{gkr} \tag{12}$$

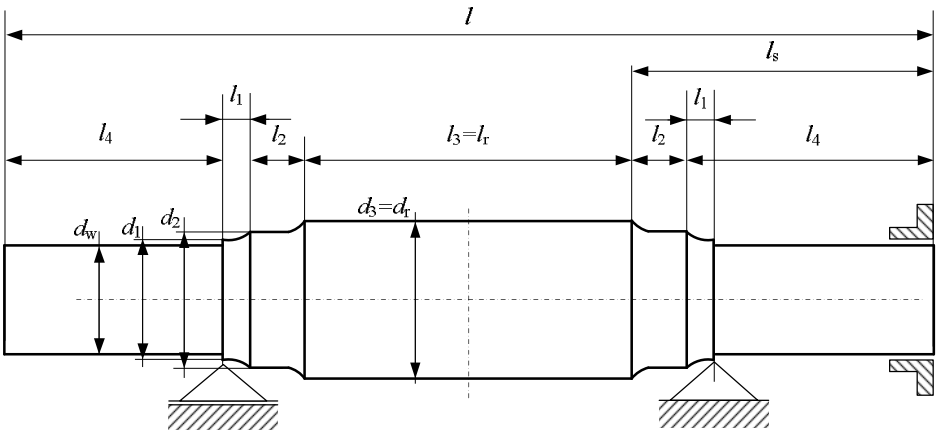

Fig. 4. Rotor dimensions of high speed PM BLDC motor
Rys. 4. Wymiary wirnika wysokoobrotowego silnik PM BLDC

3. ROTOR'S TORSIONAL VIBRATIONS

The shaft of electrical machine (including motor) is always loaded with torsional torque, on account of the principle of operation. When shaft is designed, the natural frequency of torsional vibrations ω_{os} must be determined ($\omega_{os} = \omega_{kr}$). It must be noted that in case of torsional vibrations a dangerous range of operation is the one corresponding to $0.5\omega_{os}$, in particular when the shaft is not balanced properly. By the theory of vibrations [7], natural frequency of vibrations for shaft pictured in Fig.4 may be calculated from equation:

$$\omega_{os} = \sqrt{\frac{c_s}{\Theta}} \tag{13}$$

where:

c_s - torsional rigidity of shaft,

Θ_w – mass moment of inertia.

$$\Theta_w = \frac{mr^2}{2} \tag{14}$$

where:

m – mass suspended at the rotor shaft, expressed in kg,

r – rotor shaft expressed in mm.

Torsion of the shaft in the range of elastic strains may cause (in some cases) incorrect performance of the machine. Torsion of the shaft is estimated by torsional angle φ expressed

either in radians or in degrees. For a round and smooth (or almost smooth) shaft this torsional angle φ is calculated from the relationship:

$$\varphi = \frac{M_s \cdot l_s}{I_o \cdot G} \tag{15}$$

where:

φ - torsional angle in arc measure,
M_s – torsional torque of motor shaft,
l_s – length of motor shaft,
I_o – polar moment of inertia,
G - coefficient of transverse elasticity (Kirchhoff coefficient, for steel $8.5 \cdot 10^4$ MPa).

When Eq.(15) is transformed, relationship for torsional rigidity of the shaft is obtained:

$$c_s = \frac{M_s}{\varphi} = \frac{I_o \cdot G}{l_s} \tag{16}$$

In case of stepped shafts with successive diameters d_i ($i = 1, 2, 3, \ldots n$), which correspond to lengths l_i , torsional angle is the sum of angles calculated for different shaft segments:

$$\varphi = \sum_i^n \varphi_i = \sum_i^n \frac{M_s}{c_{si}} \tag{17}$$

where:

φ_i - torsional angle of different shaft segments $l_1, l_2, l_3, \ldots l_n$,
c_{si} - torsional rigidity corresponding to successive shaft segments:

$$c_{si} = G \cdot \sum_i^n \frac{I_{oi}}{l_{si}} \tag{18}$$

Similarly as in case of bending [7], the stepped shaft may be replaced with a shaft of arbitrary equivalent diameter d_z and equivalent length l_{sz} . The equivalent rigidity will correspond to rigidity of real shaft in a following way:

$$c_{sz} = \frac{G \cdot I_{oz}}{l_{sz}} = \sum_i^n c_{si} = G \cdot \sum_i^n \frac{I_{oi}}{l_{si}} \tag{19}$$

where:

I_{oz} – equivalent polar moment of inertia of motor shaft

$$I_{oz} = \frac{\pi \cdot d_z^4}{32} \tag{20}$$

l_{sz} – equivalent length of stepped shaft, subjected to torsion at length l_s (Fig. 4):

$$l_{sz} = d_z^4 \sum_i^n \frac{l_i}{d_i^4} \tag{21}$$

It has been assumed that shaft of discussed PM BLDC motor is subjected to torsion at length l_s (Fig. 4):

$$l_s = l_1 + l_2 + l_4 \tag{22}$$

3. LABORATORY TESTS

Research aimed at developing a high-speed brushless dc motor with speed attaining 100000 rpm is ongoing in the Department of Power Electronics, Electrical Drives and Robotics of the Silesian University of Technology. During the project different issues such as design of magnetic and electrical circuit, control and supply, and impact of various electrical, mechanical and other factors on properties of high-speed PM BLDC motor have been investigated [1, 2, 3, 5].

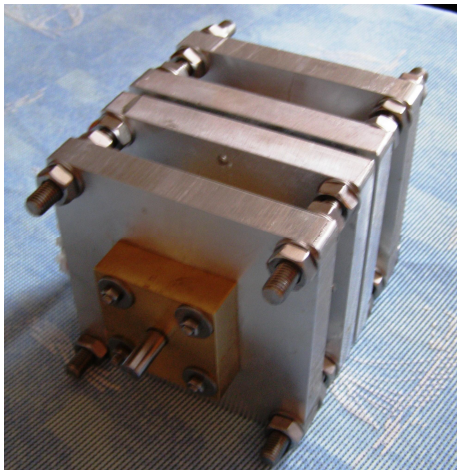

Rys. 5. Prototyp wysokoobrotowego bezszczotkowego silnika prądu stałego PM BLDC oznaczony jako silnik odniesienia (silnik I)

Fig. 5. Prototype of high-speed brushless DC motor (PM BLDC) denoted as a reference (motor I)

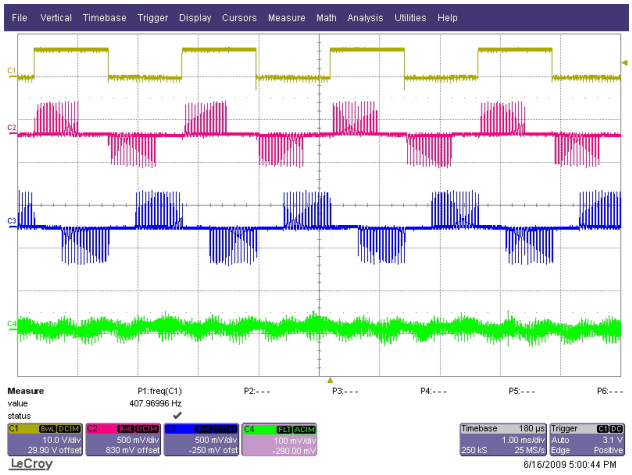

Rys. 6. Przebieg sygnału z czujnika Halla, prądów fazowych oraz sygnał z czujnika drgań nieobciążonego silnika wirującego z prędkością 24 420 obr/min (407 Hz)

Fig. 6. Waveform of Hall sensor signal, waveforms of phase currents and waveform from vibration sensor for unloaded motor rotating at 24420 rpm (407 Hz)

In the course of the project, several designs of motors of different sizes, electrical parameters and magnetic circuit constructions have been developed. It was therefore possible to evaluate several models and to select the best solution. A motor with rotor diameter d_r = 35.5 mm and length l_r = 194 mm was one of the earliest prototypes (Fig.5). This motor is now treated as a reference motor and denoted in subsequent discussion as motor I. During tests we measured (among other quantities) the motor vibrations in idle run and at speeds in the range up to 66000 rpm (Fig. 6). When rotational speed was increased above this value, resonant vibrations appeared. Piezoelectric vibration transducer located in PM BLDC motor stator was used to record vibration waveforms of the motor.

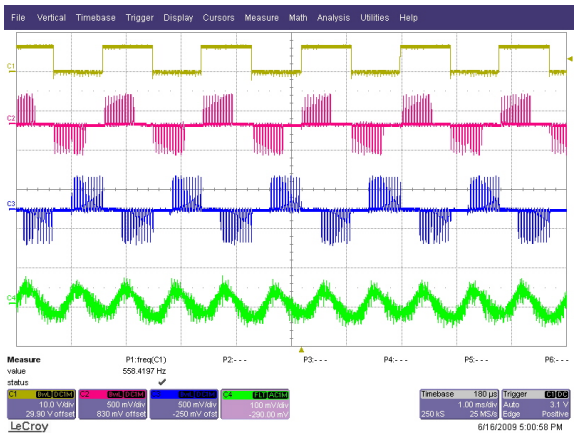

Rys. 7. Przebieg sygnału z czujnika Halla, prądów fazowych oraz sygnał z czujnika drgań nieobciążonego silnika wirującego z prędkością 33 480 obr/min (558 Hz)

Fig. 7. Waveform of Hall sensor signal, waveforms of phase currents and waveform from vibration sensor for unloaded motor rotating at 33480 rpm (558 Hz)

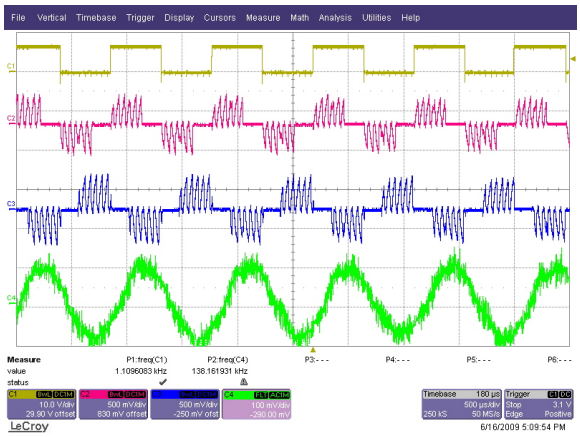

Rys. 8. Przebieg sygnału z czujnika Halla, prądów fazowych oraz sygnał z czujnika drgań nieobciążonego silnika wirującego z prędkością 66 540 obr/min (1109 Hz)

Fig. 8. Waveform of Hall sensor signal, waveforms of phase currents and waveform from vibration sensor for unloaded motor rotating at 66540 rpm (1109 Hz)

At speed approaching *c.* 33500 rpm mechanical vibrations characterized by insignificant amplitudes appeared. When speed was increased, these vibrations vanished and appeared again at speeds equal and slightly greater than 66500 rpm. Vibration waveforms are shown in Figs. 7 and 8. Apart from the vibrations, output signals from position sensors (Hall effect sensors) are shown as well as waveforms of two motor phase currents.

Table 1

Results of calculating resonant frequency for flexural vibrations

Parameter	Motor I (long rotor)	Motor II (short rotor)
Changed motor dimensions (Fig.4)	$d_{10}, l_{10},$ d_{r0}, l_{r0}	$l_{1k} < l_{10}$ $l_{rk} = l_{10}$ $d_{rk} < d_{r0}$
Equivalent rotor length l_{zg} [mm]	67.6	9.03
Moment of inertia I [mm^4]	1018	491
Shaft rigidity c_g [N/mm]	16543	3358563
Critical angular speed ω_{gkr} [1/s]	7553	115906
Critical rotational speed n_{gk} [rpm]	72124	1106823
Resonance range [rpm]	61000 ÷ 83000	94000 ÷ 127000

The waveforms (Fig.7) show that one resonance area occurred for speed equal to *c.* 33 500 rpm (this is a submultiple of critical speed). The second resonance area with higher amplitude of vibrations occurred for critical speed. The selected results of calculations characterizing the performance of the investigated motor operating in resonance area are set out in Table 1, column 2.

Since we wanted to increase range of motor's rotational speeds (above 60000 rpm), we decided to amend rotor dimensions (by slightly decreasing rotor diameter) and to decrease distance between bearings. When these quantities were changed, parameters characterizing resonance properties assumed values displayed in the third column of Table 1. A prototype of motor with changed dimensions was built and tested. Resonance vibrations did not appear even with rotational speed greatly exceeding 66000 rpm. Frequency of mechanical resonance for motor with reduced dimension was much higher than required rotational speed (equal to 100000 rpm). During lab tests we also found that the range of mechanical resonance was outside 100000 rpm.

Table 2

Results of calculating resonant frequency for torsional vibrations

Parameter	Motor I (long rotor)	Motor II (short rotor)
Changed motor dimensions (Fig. 2)	d_{10}, l_{10}, d_{r0}, l_{r0}	$l_{1k} < l_{10}$ $l_{rk} = l_{10}$ $d_{rk} < d_{r0}$
Length over which shaft is subjected to torsion l_s [mm]	77	29
Equivalent rotor length l_{zs} [mm]	116.5	24.3
Equivalent polar moment of inertia I_{oz} [mm^4]	2035	981
Torsional rigidity of the shaft c_{sz} [N/mm]	3432331	1484980
Mass moment of inertia Θ_w [kgmm^2]	48648	30157
Critical angular speed ω_{os} [1/s]	174	337
Critical rotational speed n_{gk} [rpm]	1668	3222
Resonance range [rpm]	1418 ÷ 1918	2739 ÷ 3705

Apart from flexural vibrations, torsional vibrations may also take place in a motor. The quantities describing torsional vibrations together with speeds at which resonance of torsional vibrations occurs are displayed in Table 2. For both motors (motor I – with long rotor, motor II – with shortened rotor) the range of resonance speed is much less than 4000 rpm. This is significantly lower than the proposed maximum speed of 100000 rpm and also than the submultiples of critical speed. Tests were run for speeds lower than 4000 rpm and no problems with motor performance transpired. Therefore we decided not to analyse the impact of torsional vibrations on properties of high speed PM BLDC motors.

6. CONCLUSIONS

The conducted lab tests have shown that it is possible to determine range of resonance rotational speeds caused by flexural and torsional vibrations on the basis of theoretical calculations. Analysis of test results shows that when rotor length is increased, the rotor vibration frequency decreases. In case of typical motors this effect is usually harmless, and quite often it is not even evident. In case of high-speed motor and when rotor rotates at high speed, it may happen that natural vibration frequency will be lower than rated (nominal) speed of the motor. This means that resonance may emerge and as a result motor may be damaged.

Design of electrical machine or electrical motor should focus at developing constructions where forced frequency would differ from natural frequency of the rotor. If resonance should

appear in the range of operational speeds, one of the ways of dealing with this situation is change of rotor dimensions. This method was used in the design of high-speed PM BLDC motor. However, in general rotor dimensions are not changed; instead, solutions aimed at decreasing vibrations' magnitudes are applied. Different types of dampers, shock absorbers, vibration eliminators or devices dissipating vibration energy (and diminishing vibration amplitudes and in some degree, natural vibration frequency) are built into the system. In mechanical engineering a specific role in damping vibrations is played by flexible couplings. In particular, when rubber flexible elements are used in such couplings, dynamic characteristic of the system is changed (natural frequency) and good damping properties are achieved.

REFERENCES

1. Dąbrowski M.: Projektowanie maszyn elektrycznych prądu przemiennego. Wydawnictwo Naukowo Techniczne, Warszawa 1994.
2. Gałuszkiewicz Z, Krykowski K, Miksiewicz R., Hetmańczyk J.: Wysokoobrotowy silnik PM BLDC. „Przegląd Elektrotechniczny" 2010, nr 2, s. 160-163.
3. Gałuszkiewicz Z., Krykowski K., Hetmańczyk J., Skoć A.: Rezonans mechaniczny w wysokoobrotowym silniku PM BLDC. „Zeszyty Problemowe - Maszyny Elektryczne BOBRME KOMEL" 2010, Nr 86, s. 123-128.
4. Hetmańczyk J., Krykowski K., Gałuszkiewicz Z., Miksiewicz R., Makieła D.: Wysokoobrotowy silnik wzbudzany magnesami trwałymi. „Zeszyty Problemowe - Maszyny elektryczne BOBRME KOMEL" 2010, Nr 86, s. 129-134.
5. Krykowski K., Hetmańczyk J., Skoć A.: Wpływ wymiarów wirnika na wybrane właściwości wysokoobrotowego bezszczotkowego silnika prądu stałego. „Zeszyty problemowe – Maszyny elektryczne BOBRME KOMEL" 2014, Nr 1, s. 43-48.
6. Krykowski K.: Silnik PM BLDC w napędzie elektrycznym analiza, właściwości, modelowanie. Wydawnictwo Politechniki Śląskiej, Gliwice 2011.
7. Skoć A., Spałek J., Markusik S.: Podstawy konstrukcji maszyn, Tom 2. Wydawnictwa Naukowo-Techniczne. Warszawa 2008.

Dr inż. Janusz HETMAŃCZYK, Prof. dr hab. inż. Krzysztof KRYKOWSKI
Silesian University of Technology
Faculty of Electrical Engineering, Institute Department of Power Electronics, Electrical Drives and Robotics
ul. Krzywoustego 2
44-100, Gliwice
e-mail: janusz.hetmanczyk@polsl.pl
e-mail: krzysztof.krykowski@polsl.pl

Prof. dr hab. Inż. Antoni SKOĆ
Silesian University of Technology
Faculty of Mining And Geology, Institute of Mining Mechanisation
ul. Akademicka 2
44-100 Gliwice